Journal of Clinical Monitoring and Computing (2019) 33:647–656
https://doi.org/10.1007/s10877-018-0214-4

ORIGINAL RESEARCH

Respiratory measurement using infrared thermography and respiratory volume monitor during sedation in patients undergoing endoscopic urologic procedures under spinal anesthesia

Jeongmin Kim[1] · Jun Hwan Kwon[2] · Eungjin Kim[1] · Sun Kook Yoo[2] · Cheung-soo Shin[1,3]

Received: 27 March 2018 / Accepted: 30 October 2018 / Published online: 14 November 2018

Abstract
We aimed to evaluate changes in respiratory pattern after sedation by simultaneously applying a respiratory volume monitor (ExSpiron1Xi, RVM) and infrared thermography (IRT) to patients undergoing spinal anesthesia during endoscopic urologic surgeries. After spinal anesthesia was performed, the patient was placed in a lithotomy position for surgery. Then, we established the baseline of the RVM, and started monitoring the mouth and nose with the infrared camera. SpO_2 was continuously measured throughout these processes. Once the baseline was set, 0.05 mg/kg midazolam was administered for sedation. Apnea was defined as cessation of airflow for ≥ 10 s with respiratory rate of <6 breaths/min; hypopnea was defined as a decrease in oxygen hemoglobin of $>4\%$, compared to baseline. We measured the time at which apnea was detected by IRT, the time at which hypopnea was detected by RVM, and the time at which hypoxia was detected by SpO_2. Twenty patients (age: 68.9 ± 11.2 years, body mass index: 24.2 ± 2.6 kg/min^2) completed the study. Before sedation, the baseline correlation coefficient of respiratory rate detection between RVM and IRT was 0.866. After midazolam administration, apnea was detected in all subjects within the first 5 min by IRT; the median time required to detect apnea was 102.5 [interquartile range (IQR) 25–75%: 80–155] s. Hypopnea was detected in all subjects within the first 5 min by RVM: the median time required to detect hypopnea was 142.5 (IQR 115–185.2) s. The median time required for SpO_2 to decrease $>4\%$ from baseline was 160 (IQR 125–205) s. Our results suggest that IRT can be useful for rapid detection of respiratory changes in patients undergoing sedation following spinal anesthesia for endoscopic urologic procedures.

Keywords Apnea · Intraoperative · Minute ventilation · Monitoring · Spinal anesthesia · Thermography

1 Introduction

Spinal anesthesia is commonly performed in patients undergoing endoscopic bladder or prostate resection. It provides adequate anesthesia for patients, with adequate relaxation of the pelvic floor and the perineum for the surgeon [1]. However, patients undergoing surgery under conscious spinal anesthesia experience anxiety and discomfort during the procedures, and anesthesiologists administer sedatives to reduce the discomfort [2]. Endoscopic urologic procedures require a short operation time (< 1 h); thus, anesthesiologists use an intermittent short-acting benzodiazepine as a sedative for relieving patient discomfort during the procedure. Benzodiazepines reduce minute ventilation in proportion to the dose administered. Decrease in minute ventilation leads to increase in blood carbon dioxide partial pressure, which could lead to vasodilation, tachycardia, arrhythmia—which can result in unconscious confusion—and coma. Especially in older obese male patients who are high risk of obstructive sleep apnea, a small dose of benzodiazepine may cause airway obstruction, resulting in hypoxia [3–5]. Therefore, during endoscopic procedures, the medical staff should closely observe for respiratory and cardiopulmonary complications

✉ Sun Kook Yoo

✉ Cheung-soo Shin
CHEUNG56@yuhs.ac

[1] Department of Anesthesiology and Pain Medicine, Yonsei University College of Medicine, Seoul, South Korea

[2] Department of Medical Engineering, Yonsei University College of Medicine, Seoul, South Korea

[3] Department of Anesthesiology and Pain Medicine, Anesthesia and Pain Research Institute, Yonsei University College of Medicine, 50 Yonsei-ro, Seodaemun-gu, 120-752 Seoul, South Korea

caused by sedation and be prepared to initiate prompt management of such complications [6].

As a routine practice, sedation is performed while attaching and monitoring the pulse oximetry to the patient. However, there is a definite limit to early detection of apnea by using only a pulse oximeter. The pulse oximeter works on the principle of analysis of the oxygen dissociation curve of oxygenated hemoglobin. Even if the oxygen saturation falls sharply and the oxygen partial pressure of the blood drops to 60 mm Hg, the level of oxidized hemoglobin can be kept high and the hypoxia may not be immediately detected. In contrast, it is known that the measurement of real-time end-tidal carbon dioxide partial pressure is faster and more accurate than pulse oximetry for more timely evaluation of the degree of ventilation of a patient. However, end-tidal CO_2 partial pressure is a qualitative measure, rather than a quantitative one, because this measurement yields inconsistent values in patients who exhibit spontaneous breathing without intubation [7–9].

Recently, numerous studies have been conducted to measure respiratory mechanics in a noninvasive manner. Thoracic impedance [10], acoustic monitoring [11–13], strain gauges, and magnetometers [14] have been developed. Non-invasive, non-contact imaging techniques have also been developed, including thermal imaging [15–22], structured light plethysmography [23, 24], and optoelectronic plethysmography [25, 26].

The respiratory volume monitor (RVM), which is becoming increasingly popular among the many noninvasive respiratory monitoring methods, is a tool that measures the minute ventilation, tidal volume, and respiratory rate per min in succession through a set of standard chest electrodes. Previous studies have demonstrated the accuracy of the standard spirometry measurements obtained using an RVM [27–29]. In a study on spontaneously breathing patients, the RVM's measurements of the respiratory rate demonstrated a bias of 1.8% and a relative error of 1.8% [28]. It has been shown that the RVM can be useful for real-time detection of the decrease in the minute–minute volume after sedation for spontaneous breathing for gastrointestinal endoscopic procedures [27].

The objective of this study was to determine whether an infra-red camera can detect apnea in patients undergoing spinal anesthesia during endoscopic urological surgery. In addition, we compared the speed with which IRT can detect respiratory changes, compared with RVM.

2 Method

2.1 Clinical setting

The present study was performed at Severance Hospital from February 2017 to July 2017. This study was conducted in accordance with principles of Good Clinical Practice and was approved by the Institutional Research Board of Severance Hospital (Reference No. 1-2016-0008); all patients gave written informed consent. The study was registered at ClinicalTrails.Gov with the number NCT02993497.

Twenty patients who had ASA physical status I or II and were scheduled to undergo elective transurethral resection of the prostate (TURP) or transurethral resection of the bladder (TURB) were recruited. Exclusion criteria included infection on puncture sites, coagulopathy disorders, allergy to local anesthetics, psychiatric history, and neurological diseases.

2.2 Spinal anesthesia

No premedication was given. Prior to spinal block, 300 ml of lactated Ringer's solution was administrated intravenously. Spinal puncture was performed with a 25 gauge Quincke needle at L3/4 in the lateral decubitus position. After confirmation of free-flow and clear cerebrospinal fluid, 7–8 mg of hyperbaric bupivacaine (Marcaine®Spinal Heavy: Astra, Sodertalje, Sweden) was administered intrathecally over 10–15 s. Then, the pin-prick test was performed every 2 min at the mid-thoracic line bilaterally. The peak block level was defined as the same block level that persisted at four consecutive pin-prick tests. When the peak sensory block was determined, the degree of motor block was assessed using a modified Bromage Scale (0 = no paralysis; 1 = unable to raise extended leg; 2 = unable to flex knee; 3 = unable to flex ankle) [30].

After the patient was placed in the lithotomy position for surgery, a pre-calculated (0.05 mg/kg) amount of midazolam was administered [1]. Blood pressure was monitored non-invasively and heart rates were recorded every 5 min during anesthesia, at the end of surgery, as well as at arrival and 30 min after arrival in the post anesthetic care unit. SpO_2 data were acquired every 2 s by using Masimo Radical-7®Pulse CO-Oximetry (Rad7; Masimo Corp., Irvine, CA, USA).

For real time monitoring of respiratory rate, we used non-invasive respiratory volume monitor (RVM: ExSpiron™, Respiratory Motion, Inc., Waltham, MA). The non-invasive RVM is based on thoracic electrical impedance. The impedance signal was recorded via the electrode PadSet, which was placed on the subject's thoracic region at the sternal notch, xiphoid, and mid-axillary line at the level of the xiphoid, according to manufacturer's specifications (Fig. 1).

To obtain a thermal image of fluctuations in the region around the nostrils during the respiratory cycle, as assessed by infrared thermography (IRT), the camera was placed 50 cm above the face of the patient lying down (Fig. 2). The camera has a spatial resolution of 320×240 and has a noise equivalent temperature difference (NETD) of 0.05 K (FLIR T-420, FLIR Systems, Inc). The thermal image of the patient's face, including the nasal cavity and nostril, is taken at a distance of at least 50 cm, at 10 frames/s. Imaging was performed by using a program

Fig. 1 RVM pad attached to the anterior chest with the patient in the lithotomy position for the endoscopic urologic procedure

made with the SDK (C++ ActiveX) provided by FLIR, which stores the absolute temperature as a csv file up to the second decimal place. The program was run on a work station with an i7-5500U, 8 GB RAM environment.

Figure 3 depicts the processing flowchart. First, preprocessing was performed to convert absolute temperature value to image pixel value. Second, a tracking process was performed, comprising KLT and block matching. Regions of interest (ROIs), extracted from the image domain, were obtained by KLT tracking, which compensated for large motion (i.e., head movement from respiration). In particular, a state of hypopnea causes head movement. ROIs were defined in relation to the area of respiration, which constitutes the temperature-changing region caused by respiration. Regions of measurement (ROMs), extracted from ROI sequences, were acquired by block matching, which compensated for the inaccuracy of KLT tracking. ROMs are the areas required for actual calculation. The KLT tracks head movement, enabling the ROIs to include the ROMs; the KLT extracts ROMs by using block matching. Last, respiration waveforms were extracted from ROM sequences by min–max calculating.

2.3 Pre-processing

The first step of Fig. 3 is an image preprocessing-based algorithm for respiratory rate detection, which is presented in this paper. When a temperature value must be converted to the image domain to perform image tracking, the objective of preprocessing is to maintain facial temperature characteristics for stable KLT tracking. According to the algorithm, a two-dimensional array of absolute temperature values is obtained in the subject with stable motion. The resulting temperature value includes the temperature of the nasal structure. Raw temperature value is not suitable for image processing. Therefore, the median value of the temperature value per frame is converted into the intermediate value of the 8-bit grayscale image. This conversion enables image processing while preserving the features of the facial structures to the maximum extent. The transformed image has the same coordinate values as the original data; KLT tracking is performed in the image domain, and the actual calculation is performed in the temperature domain.

The formula for the preprocessing process is shown in Eq. (1), where a is a parameter that determines the width of the temperature band to be used, depending on the experimental environment from which the temperature data is obtained. In this study, we used 0.05, which is the temperature resolution of the camera. The lower limit image pixel value has a value of 0 in an 8-bit grayscale image; and the upper limit value has a value of 255. The values between the upper and lower limits are transformed by using Eq. (2). Importantly, the median value is robust to outliers that can occur when obtaining temperature data. Outliers, such as a surgical device or doctor's actions, involve a very different temperature from that of a normal frame; thus, these change the temperature distribution of the frame. Interference of outliers can cause feature points to be lost at the moment of interference in successive image domains. Figure 4 shows that median values are more robust to outliers, compared with maximum and minimum values.

$$\begin{aligned} \text{Lower limit}_N &= \text{Median}\left(T_N(x,y)\right) - \alpha \times 128 \\ \text{Upper limit}_N &= \text{Median}\left(T_N(x,y)\right) + \alpha \times 128 \end{aligned} \tag{1}$$

$$I_N = \begin{cases} T_N(x,y) < \text{Lower limit}_N = 0 \\ \text{Lower limit}_N \le T_N(x,y) \le \text{Upper limit}_N = \frac{T_N(x,y) - \text{Lower limit}_N}{\alpha \times 256} \times 256 \\ T_N(x,y) > \text{Upper limit}_N = 255 \end{cases} \tag{2}$$

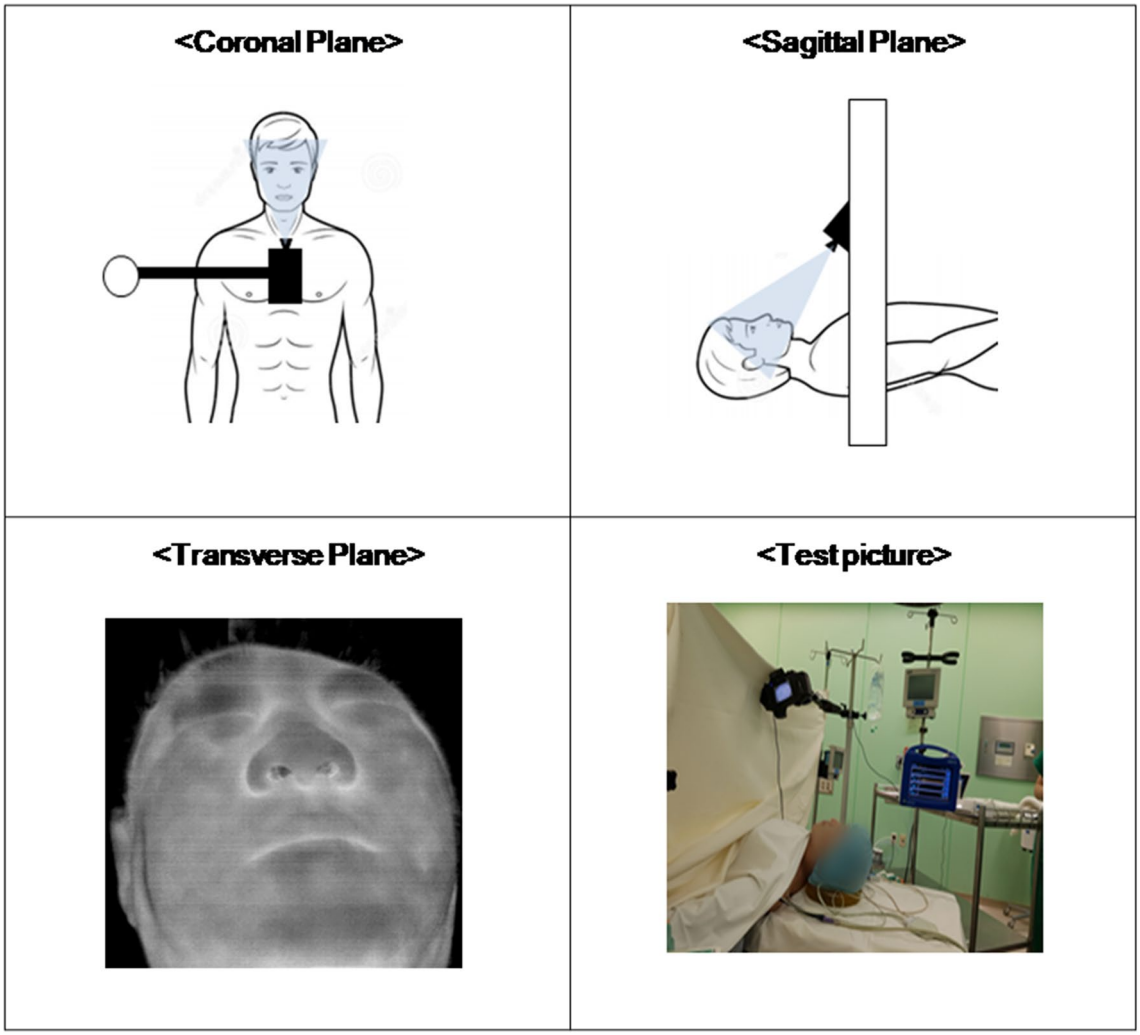

Fig. 2 Location of infrared camera installation over the subjects who underwent urologic endoscopic procedures

Fig. 3 Processing flowchart

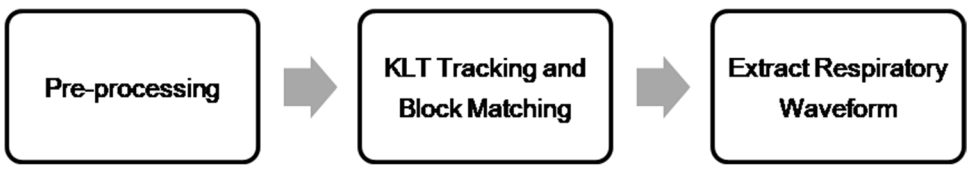

2.4 KLT tracking

The KLT Tracker (Kanade–Lucas–Tomasi) is based on the feature tracker and uses the sum of squared intensity differences matching technique to obtain a transformation matrix [31, 32]. The KLT algorithm is widely used tracking features from frame to frame [33–36]. In particular, Bourel suggests that the nostril can be used as an important anchor point in facial features [37]. In this study, the aim of tracking was to align irregular movements of the face caused by apnea. If there is an initial rotation based on the first image converted to grayscale for image processing, the nose is vertically aligned on the x and y axes by applying the initial angle to the affine transformation. The ROI is defined as including the entire nasal structure for feature extraction required for tracking. The "mineigen features" were extracted from the specified ROIs, and this was done using the "detect mineigen" function of MATLAB (version 2016b) program. The quality parameters used in the function were changed for each subject, and the optimal parameters were selected to

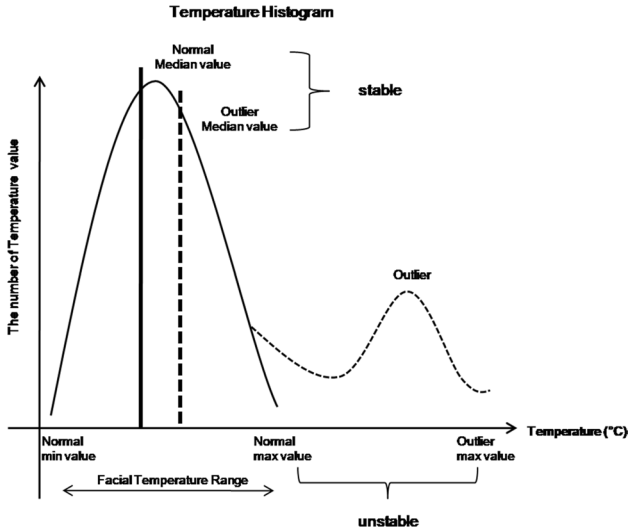

Fig. 4 Comparison of preprocessing between median and mean temperature when outliers are present in the data

perform feature extraction. Four parameters were changed to perform KLT tracking well: the number of image pyramids that change the image resolution to find larger motion [38], the threshold value of the bidirectional error when the feature disappears [39], the range value at which each feature can move between frames, and the maximum iteration counts. Figure 5 shows an example of a KLT trace. (a) shows the state where the ROM is initialized in the first image frame. (b), (c), and (d) show the process in which the ROM is tracked and aligned, on the basis of the patient's large motion.

The KLT tracking in thermal images of the face differs from the tracking in conventional RGB images. In contrast to conventional RGB images, portions of contrast that can be used as good feature points, such as lines, corners, and edges, are clear. Conversely, in thermal images of the face, the contrast is not shown because the temperature distribution is shown. To resolve this problem, median value image transformation was performed to stably extract feature points in successive image sequences during processing. This conversion stably preserves the temperature characteristics of the facial structure, allowing stable tracing even at less suitable feature points.

2.5 Block matching and extract graph

The goal of block matching is to obtain a well-aligned image for the actual calculation in a roughly aligned image. The region of measurement (ROM) is set to the position where the temperature change related to respiration is best observed in the first frame of the tracked image sequence. In this experiment, the nostril region is the ROM. We set this as the reference ROM and searching

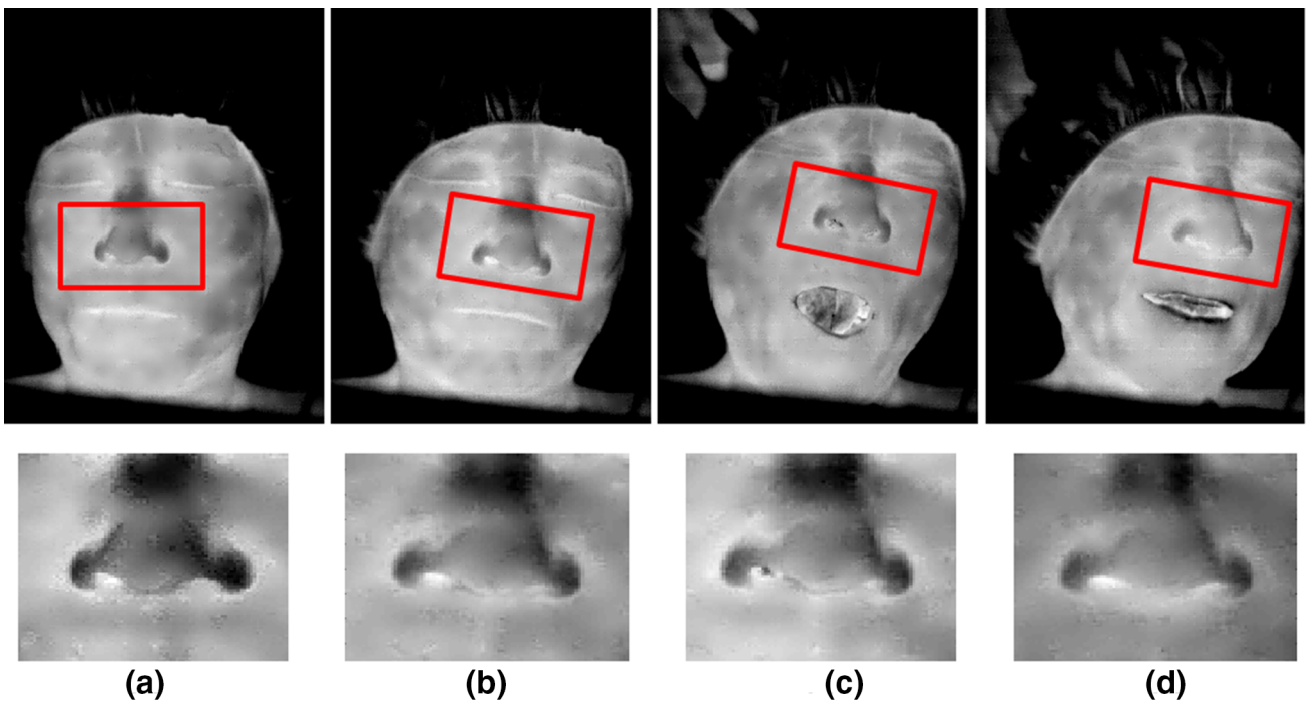

Fig. 5 The KLT Tracking (Kanade–Lucas–Tomasi) sequence example. **a** Initial frame, **b** 552 frame, **c** 561 frame, **d** 603 frame. Thermal images are captured at 10 frames/s

window of the same size to find the position where the sum of the absolute differences is the minimum and set it as the next reference ROM. Since the maximum and minimum temperatures fluctuate during the respiratory cycle, observing the tendency of max–min temperature can reveal the respiratory rate. Figure 6 shows an example of block matching. (a) shows an example of reference and searching windows in block matching. (b) Explains representative results of difference values of multiple searching windows, compared with the reference window. (1) demonstrates a low value, and (2) shows a high value. Similar to the previous reference window, this method reveals a distribution with low variance (Fig. 7).

Apnea was defined as cessation of airflow for ≥ 10 s with a respiratory rate of < 6 breaths/min, and hypopnea was defined as a decrease in oxygen hemoglobin of > 4%, compared to baseline [40]. We recorded the time when apnea was detected using the two devices, RVM and IRT. In addition, the time at which SpO_2 decreased by more than 4% compared to baseline was recorded. When hypoxemia (SpO_2 < 90%) was detected, the patient was immediately awakened to induce spontaneous breathing and additional oxygen was provided through a facial tent mask.

2.6 Statistical analysis

Statistical analysis was performed with SAS (version 9.4, SAS Inc., Cary, NC, USA) and R (version 3.4.3; http://www.R-project.org). Regarding demographic data, values are expressed as mean ± standard deviation (SD), median (95% confidential interval), or as integers (for count data). For validation of IRT for the detection of respiratory rate per min, intra-class correlation between RVM and IRT was used. Because we applied all three methods simultaneously

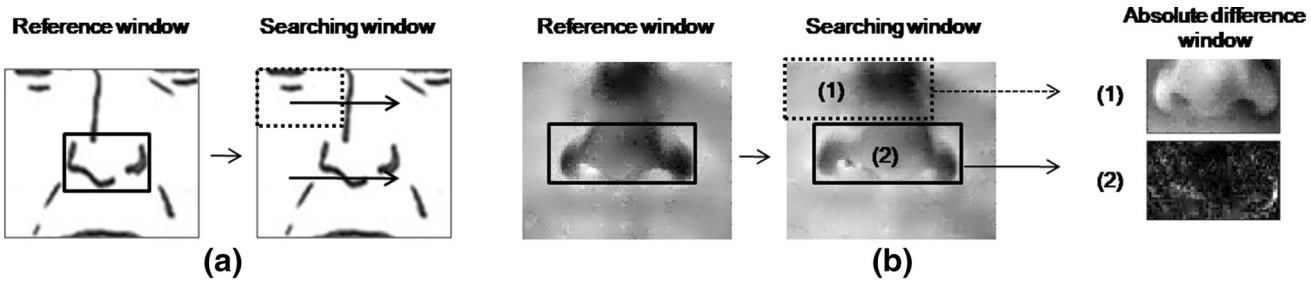

Fig. 6 Block Matching Process. **a** An example of reference and searching windows in block matching. **b** Representative results of difference values of multiple searching windows, compared with the reference window. (1) Demonstrates a low value, and (2) shows a high value

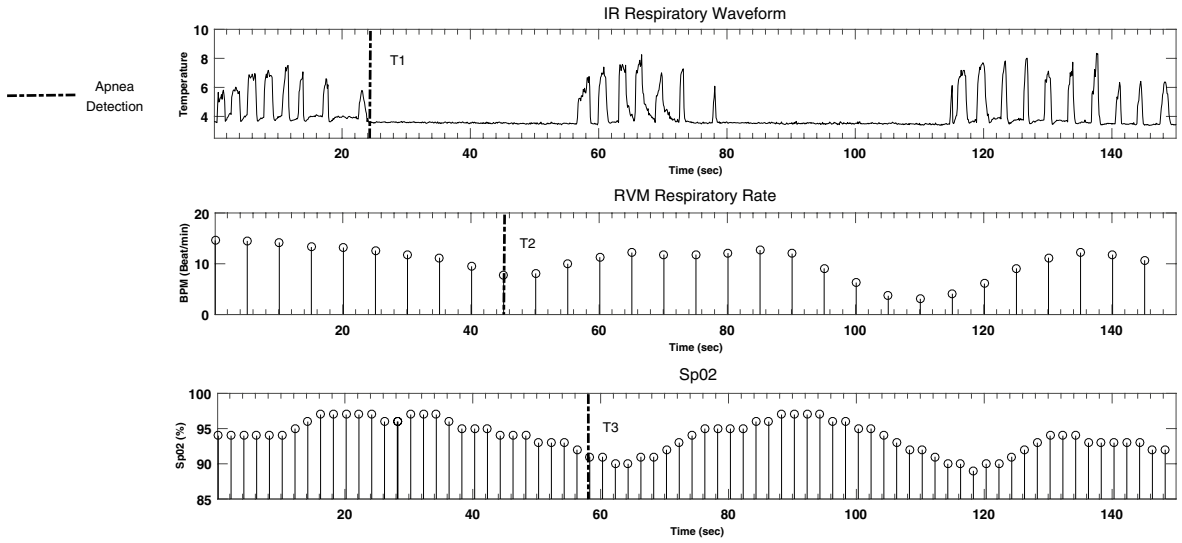

Fig. 7 Schematic representation of T1, T2, and T3 in a representative subject. T1, Time required to observe apnea by IRT camera after midazolam injection; T2, Time required to observe apnea by RVM after midazolam injection; T3, Time required for SpO_2 to decrease after midazolam injection

to one patient, we analyzed by using the stratified log-rank test, rather than the unmodified/standard log-rank test. The overall test was performed comparing among the three methods; pairwise comparisons were performed with Bonferroni correction. In addition, since T1, T2, and T3 did not follow normal distributions, the overall difference was tested by the non-parametric Friedman's test; pairwise tests were performed with Wilcoxon's signed rank tests. Similarly, multiple comparisons were adjusted using Bonferroni correction.

3 Results

Twenty patients (19 males, 1 female) were enrolled in this pilot study (Table 1). All subjects underwent urologic endoscopic procedures (TURP or TURB). The mean age of subjects was 68.9 ± 11.2 years, and mean body mass index of the subjects was 24.2 ± 2.6 kg/min^2. The mean dose of bupivacaine administered for spinal anesthesia was 7.8 ± 1.0 mg. All subjects received 0.05 mg of midazolam per kg after spinal anesthesia (Table 1. mean ± SD; 3.16 ± 0.41).

3.1 Correlation of RVM and IRT

Correlation between respiratory rate measured with two devices (RVM and IRT) was determined by intra-class correlation before midazolam administration. We obtained respiratory rate measurement by two methods, RVM and infrared, measured for 30 s in each patient. Therefore, we considered repeated measures when estimating the correlation between the two methods. The correlation coefficient between RVM and infrared with repeated measures was r = 0.8659 ($p < 0.0001$). Figure 8 shows the Bland–Altman plot of the RR measured by RVM and infrared camera. The validation test demonstrated a strong correlation of respiratory rate measured by RVM and IRT (Table 2).

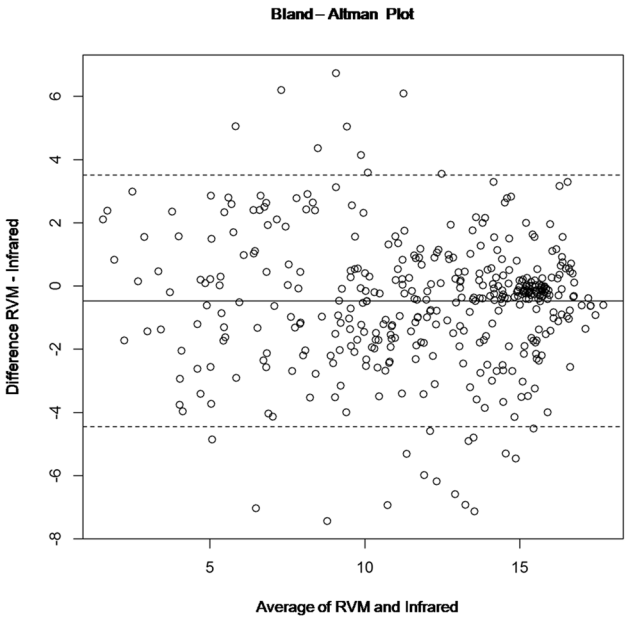

Fig. 8 Bland–Altman plot of baseline respiratory volume monitor (RVM) and infrared thermography (infrared)

3.2 Comparison of time to detection of change in breathing pattern among three different devices after midazolam administration

T1 was defined as the time at which apnea was first measured in the IRT after midazolam injection. We defined T2 as the first recorded time of < 6 breaths/min in the RVM after midazolam injection. T3 was defined as the time at which SpO_2 began to drop below baseline 4%, or 90%, after drug injection.

In all subjects, apnea was detected by IRT within the first 5 min after midazolam administration. The median time for the first observation of apnea with IRT was 102.5 s, and IRT was the fastest method of measuring apnea among the three methods. The difference was

Table 1 Patient demographics and clinical characteristics

	Mean	Standard deviation
Age (years)	68.9	11.2
Sex (male/female)	19/1	
Body mass index (kg/m^2)	24.2	2.6
Bupivacaine dose for spinal anesthesia (mg)	7.8	1.0
Midazolam dose for sedation (mg)	3.16	0.41
Peak sensory block level by spinal anesthesia (thoracic 7/8/9)	(5/5/10)	
Duration of operation (mm:ss)	41 min 26 s	12 min 15 s
TURP/TURB	(16/4)	
The difference between the maximum and minimum temperature measured by infrared thermography during respiration (°C)	3.12	0.94

TURP transurethral resection of the prostate, *TURB* transurethral resection of the bladder

Table 2 Comparison of apnea detection time measured by three methods

	Median (s)	IQR (25–75%)	Overall	T1 versus T2	T1 versus T3	T2 versus T3
T1	102.5	80–155	< 0.0001	< 0.0001**	< 0.0001**	0.005**
T2	142.5	115–185.2				
T3	160	125–205				

IRT infrared thermography, *RVM* respiratory volume monitor, *T1* Time required to observe apnea by IRT camera after midazolam injection, *T2* Time required to observe apnea by RVM after midazolam injection; *T3* Time required for SpO_2 to decrease after midazolam injection; values are median (interquartile 25–75%)

$^{**}p < 0.01$

statistically significant as determined by stratified log rank test ($p < 0.05$).

The long-link test was performed among the three methods, and the pairwise comparison results were presented with Bonferroni correction. Compared with T3, both T1 and T2 showed statistically significant differences. In addition, a statistically significant difference was also observed when T1 and T2 were compared.

4 Discussion

The results of this study show that IRT detected apnea more quickly compared to the use of RVM or evaluation of SpO_2 in patients under sedation after spinal anesthesia. Compared with evaluation of SpO_2, when IRT was used, respiratory deterioration could be detected 1 min earlier; respiratory depression could be detected 40 s earlier than when RVM was used. According to these results, IRT constitutes a rapid diagnostic tool for respiratory depression in patients who are susceptible to hypoxemia during monitored anesthesia care.

Patients undergoing surgery with spinal anesthesia are frequently sedated to suppress awareness and to enhance comfort. However, sometimes, even a small dose of benzodiazepine could cause unexpected deep sedation leading to upper airway collapse and may cause severe arterial oxygen desaturation. In this study, a novel non-invasive, non-contact respiratory monitor was used to assess the component of ventilation in endoscopic urologic procedures. The ASA practice guidelines for sedation and analgesia indicate that the primary causes of morbidity during sedation are drug-induced respiratory depression and airway obstruction [41]. The guideline recommendations for ventilation monitoring through observation or auscultation do not provide an objective measure of respiratory volumes. The inclusion of $EtCO_2$ monitoring in procedural sedation procedures performed by anesthesiologists provides a surrogate measure of ventilation; however, this monitoring technique is not always available, is not a quantitative test, and has limitations.

In recent years, contactless monitoring tools are increasingly being used, and IRT is being developed as an image diagnostic tool in various medical fields [16–22, 42–48]. According to the data in this study, in patients under conscious sedation, IRT is comparable in reliability to other non-invasive respiratory measurements, such as RVM, and could detect respiratory deterioration sooner than RVM.

The greatest limitation of this study is that this was a small-scale pilot study of 20 patients who underwent spinal anesthesia. A large-scale follow-up study is needed to determine whether respiration can be measured by applying IRT in a variety of clinical situations and patient populations. Second, we did not measure respiration quantitatively. Previous studies reported that respiratory rate-based alarm cutoff monitoring would not only fail to detect low minute ventilation events but would also capture numerous false-positive events [27]. In addition, Castro et al. reported that the respiratory depression effect of perioperative benzodiazepine influences TV, rather than RR [49]. Further research is needed to determine whether tidal volume can be measured with IRT by calibrating the patient's movements. Third, to commercialize IRT as a medical monitoring device, it is necessary to resolve the technical limitations of IRT itself. For example, it is necessary to determine whether a subtle temperature change can be detected in an environment that involves extreme temperature changes, and whether the breathing of the patient can be immediately monitored and quantified. Therefore, we think that IRT should be used as an auxiliary tool for devices that are already used in clinical situations, such as RVM. Fourth, a simple comparison of two devices with different measurement mechanisms could be problematic in itself. RVM has been validated and commercialized to measure the RR and TV of spontaneously breathing patients. However, RVM is not designed to detect apnea, but constitutes a device designed to calculate a low respiration rate over an average of 30 s. Considering the measurement principle, RVM is delayed in reporting hypopnea with respect to IRT, so it may not be fair to compare these two devices.

Notwithstanding, these limitations, the results of the present study are significant in at least two major respects. First, the IRT provides the possibility of non-contact respiratory monitoring. In addition to patients with spinal anesthesia, IRT may be a useful tool for patients in other clinical settings, such as when using sedation for CT or MRI study.

Second, this study aimed to overcome the limitations of the current respiratory monitoring tools used in clinical practice. So far, hypoxic symptoms have been treated symptomatically only when hypoxia due to respiratory depression occurs on administration of a sedative to the patient. Real-time instant respiratory monitoring systems, such as IRT, could detect apnea events before symptoms of hypoxia occur and could prevent major complications, such as respiratory arrest.

5 Conclusion

Our results suggest that IRT can be used for rapid detection of respiratory changes in patients undergoing sedation following spinal anesthesia for endoscopic urologic procedures.

Compliance with ethical standards

Conflict of interest The authors declare that they have no conflict of interest.

Informed consent Informed consent was obtained from all individual participants included in the study.

Research involving human participants All procedures performed in studies involving human participants were in accordance with the ethical standards of the institutional and/or national research committee and with the 1964 Helsinki declaration and its later amendments or comparable ethical standards.

References

1. Miller RD. Miller's anesthesia. 8th ed. Philadelphia: Elsevier/Saunders; 2015.
2. Kim J, Kim WO, Kim HB, Kil HK. Adequate sedation with single-dose dexmedetomidine in patients undergoing transurethral resection of the prostate with spinal anaesthesia: a dose-response study by age group. BMC Anesthesiol. 2015;15:17. https://doi.org/10.1186/1471-2253-15-17.
3. Deng X, Gu W, Li Y, Liu M, Li Y, Gao X. Age-group-specific associations between the severity of obstructive sleep apnea and relevant risk factors in male and female patients. PLoS ONE. 2014;9(9):e107380. https://doi.org/10.1371/journal.pone.0107380.
4. Allott EH, Masko EM, Freedland SJ. Obesity and prostate cancer: weighing the evidence. Eur Urol. 2013;63(5):800–9. https://doi.org/10.1016/j.eururo.2012.11.013.
5. Bezel R, Russi E, Kronauer H, Mothersill I. Life-threatening apnea after midazolam administration in a patient with obstructive sleep apnea syndrome. Schweiz Med Wochenschr. 1987;117(15):579–83.
6. Kiriyama S, Gotoda T, Sano H, Oda I, Nishimoto F, Hirashima T, Kusano C, Kuwano H. Safe and effective sedation in endoscopic submucosal dissection for early gastric cancer: a randomized comparison between propofol continuous infusion and intermittent midazolam injection. J Gastroenterol. 2010;45(8):831–7. https://doi.org/10.1007/s00535-010-0222-8.
7. Beitz A, Riphaus A, Meining A, Kronshage T, Geist C, Wagenpfeil S, Weber A, Jung A, Bajbouj M, Pox C, Schneider G, Schmid RM, Wehrmann T, von Delius S. Capnographic monitoring reduces the incidence of arterial oxygen desaturation and hypoxemia during propofol sedation for colonoscopy: a randomized, controlled study (ColoCap Study). Am J Gastroenterol. 2012;107(8):1205–12. https://doi.org/10.1038/ajg.2012.136.
8. Friedrich-Rust M, Welte M, Welte C, Albert J, Meckbach Y, Herrmann E, Kannengiesser M, Trojan J, Filmann N, Schroeter H, Zeuzem S, Bojunga J. Capnographic monitoring of propofol-based sedation during colonoscopy. Endoscopy. 2014;46(3):236–44. https://doi.org/10.1055/s-0033-1359149.
9. Qadeer MA, Vargo JJ, Dumot JA, Lopez R, Trolli PA, Stevens T, Parsi MA, Sanaka MR, Zuccaro G. Capnographic monitoring of respiratory activity improves safety of sedation for endoscopic cholangiopancreatography and ultrasonography. Gastroenterology. 2009;136(5):1568–76. quiz 819–20.
10. Houtveen JH, Groot PFC, de Geus EJC. Validation of the thoracic impedance derived respiratory signal using multilevel analysis. Int J Psychophysiol. 2006;59(2):97–106. https://doi.org/10.1016/j.ijpsycho.2005.02.003.
11. Corbishley P, Rodriguez-Villegas E. Breathing detection: towards a miniaturized, wearable, battery-operated monitoring system. Biomed Eng IEEE Trans. 2008;55(1):196–204. https://doi.org/10.1109/TBME.2007.910679.
12. Jafarian K, Amineslami M, Hassani K, Navidbakhsh M, Lahiji MN, Doyle DJ. A multi-channel acoustics monitor for perioperative respiratory monitoring: preliminary data. J Clin Monit Comput. 2016;30(1):107–18. https://doi.org/10.1007/s10877-015-9693-8.
13. Guechi Y, Pichot A, Frasca D, Rayeh-Pelardy F, Lardeur JY, Mimoz O. Assessment of noninvasive acoustic respiration rate monitoring in patients admitted to an emergency department for drug or alcoholic poisoning. J Clin Monit Comput. 2015;29(6):721–6. https://doi.org/10.1007/s10877-015-9658-y.
14. Avraam J, Bourke R, Trinder J, Nicholas CL, Brazzale D, O'Donoghue FJ, Rochford PD, Jordan AS. The effect of body mass and sex on the accuracy of respiratory magnetometers for measurement of end-expiratory lung volumes. J Appl Physiol (1985). 2016;121(5):1169–77. https://doi.org/10.1152/japplphysiol.00571.2016.
15. Chekmenev SY, Rara H, Farag AA. Non-contact, wavelet-based measurement of vital signs using thermal imaging. In: Proceedings of the The first international conference on graphics, vision, and image processing (GVIP), Cairo, Egypt, 2005.
16. Murthy R, Pavlidis I, Tsiamyrtzis P. Touchless Monitoring of Breathing Function. In: Proceedings of the 26th Annual International Conference of the IEEE EMBS. San Francisco, CA, USA, September 1–5, 2004.
17. Goldman LJ. Nasal airflow and thoracoabdominal motion in children using infrared thermographic video processing. Pediatr Pulmonol. 2012;47(5):476–86. https://doi.org/10.1002/ppul.21570.
18. Fei J, Pavlidis I. Virtual Thermistor. In: Proceedings of the 29th Annual International Conference of the IEEE EMBS. Cité Internationale, Lyon, France, August 23–26, 2007.
19. Murthy R, Pavlidis I, Tsiamyrtzis P. Touchless monitoring of breathing function 2004.
20. Fei J, Pavlidis I. Thermistor at a distance: unobtrusive measurement of breathing. IEEE Trans Biomed Eng. 2010;57(4):988–98. https://doi.org/10.1109/tbme.2009.2032415.
21. Abbas AK, Heimann K, Jergus K, Orlikowsky T, Leonhardt S. Neonatal non-contact respiratory monitoring based on real-time infrared thermography. Biomed Eng Online. 2011;10:93. https://doi.org/10.1186/1475-925x-10-93.
22. Pereira CB, Yu X, Czaplik M, Rossaint R, Blazek V, Leonhardt S. Remote monitoring of breathing dynamics using infrared

thermography. Biomed Opt Express. 2015;6(11):4378–94. https://doi.org/10.1364/boe.6.004378.
23. Wareham R, Lasenby J, Cameron P, Iles R. Structured light plethysmography (SLP) compared to spirometry: a pilot study. In: Proceedings of the European Respiratory Society Annual Congress, 2009.
24. Aoki H, Koshiji K, Nakamura H, Takemura Y, Nakajima M. Study on respiration monitoring method using near-infrared multiple slit-lights projection. In: Proceedings of the Micro-NanoMechatronics and Human Science, 2005 IEEE International Symposium on, 2005.
25. Aliverti A, DellacÁ R, Pelosi P, Chiumello D, Pedotti A, Gattinoni L. Optoelectronic plethysmography in intensive care patients. Am J Respir Crit Care Med. 2000;161(5):1546–52. https://doi.org/10.1164/ajrccm.161.5.9903024.
26. Cala S, Kenyon C, Ferrigno G, Carnevali P, Aliverti A, Pedotti A, Macklem P, Rochester D. Chest wall and lung volume estimation by optical reflectance motion analysis. J Appl Physiol. 1996;81(6):2680–9.
27. Holley K, MacNabb CM, Georgiadis P, Minasyan H, Shukla A, Mathews D. Monitoring minute ventilation versus respiratory rate to measure the adequacy of ventilation in patients undergoing upper endoscopic procedures. J Clin Monit Comput. 2015. https://doi.org/10.1007/s10877-015-9674-y.
28. Voscopoulos C, Brayanov J, Ladd D, Lalli M, Panasyuk A, Freeman J. Special article: evaluation of a novel noninvasive respiration monitor providing continuous measurement of minute ventilation in ambulatory subjects in a variety of clinical scenarios. Anesth Analg. 2013;117(1):91–100. https://doi.org/10.1213/ANE.0b013e3182918098.
29. Voscopoulos CJ, MacNabb CM, Brayanov J, Qin L, Freeman J, Mullen GJ, Ladd D, George E. The evaluation of a non-invasive respiratory volume monitor in surgical patients undergoing elective surgery with general anesthesia. J Clin Monit Comput. 2015;29(2):223–30. https://doi.org/10.1007/s10877-014-9596-0.
30. Bromage PR. Epidural analgesia. Philadelphia: WB Saunders; 1978.
31. Lucas BD, Kanade T. An iterative image registration technique with an application to stereo vision. 1981.
32. Tomasi C, Kanade T. Detection and tracking of point features. 1991.
33. Li H, Lu J, Shi G, Zhang Y. Tracking features in retinal images of adaptive optics confocal scanning laser ophthalmoscope using KLT-SIFT algorithm. Biomed Opt Express. 2010;1(1):31–40.
34. Lee WO, Lee EC, Park KR. Blink detection robust to various facial poses. J Neurosci Methods. 2010;193(2):356–72. https://doi.org/10.1016/j.jneumeth.2010.08.034.
35. Al-Najdawi N, Tedmori S, Edirisinghe E, Bez H. An automated real-time people tracking system based on KLT Features Detection. Int Arab J Inf Technol. 2012;9:100–107
36. Lin G, Tsai T. A face tracking method using feature point tracking. In: Proceedings of the 2012 International Conference on Information Security and Intelligent Control, 14–16 Aug. 2012.
37. Bourel F, Chibelushi CC, Low AA. Robust facial feature tracking. In: Proceedings of the BMVC, 2000.
38. Adelson EH, Anderson CH, Bergen JR, Burt PJ, Ogden JM. Pyramid methods in image processing. RCA Eng. 1984;29(6):33–41.
39. Kalal Z, Mikolajczyk K, Matas J. Forward-backward error: Automatic detection of tracking failures. In: Proceedings of the Pattern recognition (ICPR), 2010 20th international conference on, 2010.
40. Young T, Palta M, Dempsey J, Skatrud J, Weber S, Badr S. The occurrence of sleep-disordered breathing among middle-aged adults. N Engl J Med. 1993;328(17):1230–5. https://doi.org/10.1056/nejm199304293281704.
41. Anonymous. Practice guidelines for sedation and analgesia by non-anesthesiologists. Anesthesiology. 2002;96(4):1004–17.
42. Seo S, Han Y, Kim J, Choung JT, Kim BJ, Ahn K. Infrared camera-proven water-damaged homes are associated with the severity of atopic dermatitis in children. Ann Allergy Asthma Immunol. 2014;113(5):549–55. https://doi.org/10.1016/j.anai.2014.08.013.
43. Dini V, Salvo P, Janowska A, Di Francesco F, Barbini A, Romanelli M. Correlation between wound temperature obtained with an infrared camera and clinical wound bed score in venous leg ulcers. Wounds. 2015;27(10):274–8.
44. Singer AJ, Relan P, Beto L, Jones-Koliski L, Sandoval S, Clark RA. Infrared thermal imaging has the potential to reduce unnecessary surgery and delays to necessary surgery in burn patients. J Burn Care Res. 2016;37(6):350–5. https://doi.org/10.1097/bcr.0000000000000330.
45. Avetisov SE, Novikov IA, Lutsevich EE, Reyn ES. Use of infrared thermography in ophthalmology. Vestn Oftalmol. 2017;133(6):99–105. https://doi.org/10.17116/oftalma2017133699-104.
46. Owen R, Ramlakhan S, Saatchi R, Burke D. Development of a high-resolution infrared thermographic imaging method as a diagnostic tool for acute undifferentiated limp in young children. Med Biol Eng Comput. 2017. https://doi.org/10.1007/s11517-017-1749-0.
47. Hu M, Zhai G, Li D, Fan Y, Duan H, Zhu W, Yang X. Combination of near-infrared and thermal imaging techniques for the remote and simultaneous measurements of breathing and heart rates under sleep situation. PLoS ONE. 2018;13(1):e0190466. https://doi.org/10.1371/journal.pone.0190466.
48. Wild T, Becker M, Winter J, Schuhschenk N, Daeschlein G, Siemers F. Hyperspectral imaging of tissue perfusion and oxygenation in wounds: assessing the impact of a micro capillary dressing. J Wound Care. 2018;27(1):38–51. https://doi.org/10.12968/jowc.2018.27.1.38.
49. Gonzalez Castro LN, Mehta JH, Brayanov JB, Mullen GJ. Quantification of respiratory depression during pre-operative administration of midazolam using a non-invasive respiratory volume monitor. PLoS ONE. 2017;12(2):e0172750. https://doi.org/10.1371/journal.pone.0172750.